Development 129, 5499-5510

doi:10.1242/dev.00122

The divergent *C. elegans* ephrin EFN-4 functions in embryonic morphogenesis in a pathway independent of the VAB-1 Eph receptor

Ian D. Chin-Sang*,†, Sarah L. Moseley†, Mei Ding, Robert J. Harrington, Sean E. George and Andrew D. Chisholm‡

Department of Molecular, Cell, and Developmental Biology, Sinsheimer Laboratories, University of California, Santa Cruz, CA 95064, USA

*Present address: Department of Biology, Queen's University, Kingston, Ontario K7L 3N6, Canada
†These authors contributed equally to this work
‡Author for correspondence (e-mail: chisholm@biology.ucsc.edu)

Accepted 4 September 2002

SUMMARY

The *C. elegans* genome encodes a single Eph receptor tyrosine kinase, VAB-1, which functions in neurons to control epidermal morphogenesis. Four members of the ephrin family of ligands for Eph receptors have been identified in *C. elegans*. Three ephrins (EFN-1/VAB-2, EFN-2 and EFN-3) have been previously shown to function in VAB-1 signaling. We show that mutations in the gene *mab-26* affect the fourth *C. elegans* ephrin, EFN-4. We show that *efn-4* also functions in embryonic morphogenesis, and that it is expressed in the developing nervous system. Interestingly, *efn-4* mutations display synergistic interactions with mutations in the VAB-1 receptor and in the EFN-1 ephrin, indicating that EFN-4 may function independently of the VAB-1 Eph receptor in morphogenesis. Mutations in the LAR-like receptor tyrosine phosphatase PTP-3 and in the Semaphorin-2A homolog MAB-20 disrupt embryonic neural morphogenesis. *efn-4* mutations synergize with *ptp-3* mutations, but not with *mab-20* mutations, suggesting that EFN-4 and Semaphorin signaling could function in a common pathway or in opposing pathways in *C. elegans* embryogenesis.

Key words: Morphogenesis, *C. elegans*, Ephrin, Semaphorin, EFN-4, VAB-1

INTRODUCTION

The epidermis of *C. elegans* is a simple epithelium that forms the skin of the animal. Morphogenesis of the *C. elegans* epidermis provides a model for several aspects of epithelial biology, including epithelial cell fate determination, cell polarity, cell motility and cell shape (Chin-Sang and Chisholm, 2000; Michaux et al., 2001; Simske and Hardin, 2001). Epidermal cells arise on the dorsal surface of the embryo, where they form junctions to give rise to an epithelial sheet. The epidermal sheet then spreads laterally and ventrally to close up at the ventral midline, an example of epiboly referred to in *C. elegans* as epidermal enclosure (Williams-Masson et al., 1997). Epidermal enclosure itself can be divided into two steps: in the first step, two bilateral pairs of epidermal cells extend actin-rich processes over a substrate of neural cells. These processes meet their contralateral counterparts at the ventral midline, leading to the rapid formation of junctions between the two pairs of cells (Raich et al., 1999). In the second step, other epidermal cells enclose the posterior body, possibly by a supracellular actin purse-string mechanism (Simske and Hardin, 2001).

We have previously shown that the *C. elegans* Eph receptor VAB-1 and its ephrin ligand EFN-1 (previously called VAB-2) function in epidermal enclosure (Chin-Sang et al., 1999; George et al., 1998). During epidermal enclosure, VAB-1 and EFN-1 are predominantly expressed and required in underlying neurons but not in the epidermal cells. Time-lapse analysis of *vab-1* and *efn-1* mutant embryos revealed specific defects in the organization of neural precursors, manifested as a failure to close the 'gastrulation cleft', a depression in the ventral surface of the embryo left after ingression of endodermal and mesodermal precursors. Because epidermal cells migrate over the descendants of these ventral neural precursors, a simple model for the non-autonomous effects of *vab-1* or ephrin mutants on epidermal enclosure is that they arise as a consequence of an altered neural substrate. The defects in neural cell organization in *C. elegans* Eph signaling mutants may resemble cell sorting defects observed in vertebrates when Eph signaling is disrupted (Mellitzer et al., 1999; Xu et al., 2000).

The relative simplicity of the *C. elegans* Eph signaling network allows a systematic analysis of its roles in a single morphogenetic process. A single Eph receptor (VAB-1) and four ephrins (EFN-1 through EFN-4) have been identified in *C. elegans* (Wang et al., 1999). *efn-1* mutations, obtained from forward genetic screens, cause phenotypes weaker than but otherwise indistinguishable from those of *vab-1* mutants;

expression, binding and genetic data indicate that EFN-1 functions as a ligand for VAB-1 in embryonic morphogenesis (Chin-Sang et al., 1999). *efn-2* and *efn-3* mutants, obtained by reverse genetics, appear essentially normal during embryogenesis; EFN-2 is expressed embryonically in a pattern similar to EFN-1. The *efn-1* null phenotype is much weaker than that of *vab-1*, and an *efn-1 efn-2 efn-3* triple mutant resembles a *vab-1* knockout, suggesting that *efn-2* and *efn-3* play subtle roles in embryogenesis that are partly redundant with *efn-1* (Wang et al., 1999) (S. L. M. and A. D. C., unpublished) The similarity of the *efn-1 efn-2 efn-3* triple mutant phenotype to the *vab-1* null phenotype suggests that these three ephrins might account for all signaling functions of the VAB-1 Eph receptor. VAB-1/EFN-1 signaling also appears to function partly redundantly with a pathway involving the LAR-like receptor tyrosine phosphatase PTP-3 (Harrington et al., 2002).

We report our analysis of a fourth worm ephrin, EFN-4, focusing on its functions in embryonic morphogenesis. We show that EFN-4 is also required for movement of embryonic neural precursors and enclosure of the epidermis, but that its role is distinct from those of VAB-1 or EFN-1. Unexpectedly, *efn-4* mutations show strong synergistic interactions with mutations in *vab-1* and *efn-1*, suggesting that EFN-4 may function in a VAB-1-independent pathway. *efn-4* mutations also synergize with *ptp-3* mutations, suggesting that EFN-4 does not function solely in the PTP-3 pathway. Through a comprehensive analysis of *vab-1 efn* double mutants we find that only *efn-4* mutations show strong synergism with *vab-1* receptor mutants. It had been suggested that the Semaphorin-2A homolog MAB-20 might function in the EFN-4 pathway (Roy et al., 2000). We find that *efn-4* and *mab-20* mutations show either epistasis or weak mutual suppression, suggesting that these genes could act in common or opposing pathways in embryonic morphogenesis.

MATERIALS AND METHODS

Genetic analysis

C. elegans strains were cultured using standard methods, at 20°C unless stated (Brenner, 1974). Mutations used are described elsewhere (Riddle et al., 1997), in papers indicated or in this paper. Mutations used were:

LGI, *mab-20(ev574, e819, bx24)*;

LGII, *vab-1(dx31, e118, ju8, e699, e856, e1029), ptp-3(op147)* (Harrington et al., 2002);

LGIV, *dpy-9(e12), efn-1(e96, ju1, ju90)* (Chin-Sang et al., 1999), *efn-2(ev658)*; and

LGX, *efn-3(ev696)* (Wang et al., 1999).

Rearrangements used were: *mIn1 mIs14* (Edgley and Riddle, 2001); and *mDp1(IV; f)*.

All *efn-4* mutations were EMS-induced, with the exception of *bx80* (diepoxybutane). S. Brenner isolated the *efn-4* mutations *e36* and *e660*; J. Hodgkin isolated *e1746*; X. Huang isolated *ju134*. All *efn-4* alleles failed to complement *bx80*. *efn-4(ju314)*, isolated independently from *e1746*, was found to cause similar phenotypes and to result from the same molecular lesion.

e819 is an X-ray-induced mutation isolated by S. Brenner and assigned to *mab-20* by mapping and complementation tests (data not shown). *mab-20(e819)* causes embryonic and larval lethal phenotypes similar in penetrance to those of *mab-20(ev574)*, suggesting that it causes a strong loss of function. The weak *vab-1* allele *e1029* has been found to result from a mis-sense mutation (C212Y) in the extracellular domain of VAB-1. Penetrance of lethality and morphogenetic defects was quantitated as described previously (George et al., 1998); all estimates of penetrance were obtained from counts of between 3 and 6 complete broods.

Double mutant construction and analysis

vab-1(0); efn-4 double mutants were completely inviable and were maintained as balanced strains. We initially used *dpy-9* as a balancer for *efn-4*; however, such strains were unstable, owing to recombination between *dpy-9* and *efn-4*. We subsequently constructed more stable balanced strains of genotype *vab-1/mIn1 mIs14; efn-4*. *vab-1 efn-4* double homozygotes were identified as non-GFP-expressing progeny from such heterozygotes. Some *vab-1 efn-4* double mutants constructed using weak *vab-1* alleles were subviable; rare viable and fertile non-GFP-expressing progeny were identified as segregants from *mIn1 mIs14*-balanced strains. Such homozygous *vab-1 efn-4* double mutants could be propagated very slowly, and displayed >99% lethality (see Fig. 5). Some *vab-1; efn-4* double mutants were maintained as homozygous lines balanced by an extrachromosomal array (*juEx350*) carrying the wild-type copies of *vab-1* and *efn-4*. *juEx350* was formed by co-injection of the *vab-1(+)* cosmid M03A1 (1 ng/μl), the *efn-4(+)* cosmid F56A11 (1 ng/μl), the plasmid pRF4 (30 ng/μl), the SUR-5-GFP marker pTG96 (30 ng/μl) and pBluescript (40 ng/μl). *ptp-3 efn-4* double mutants and *vab-1 ptp-3 efn-4* triple mutants were analyzed from balanced strains of genotype *ptp-3* (or *vab-1 ptp-3*)*/mIn1 mIs14; efn-4*.

mab-20 efn-4 double mutants were constructed using *dpy-9* as a marker in trans to *efn-4*; all double mutants were confirmed by multiple complementation tests. We used one-way ANOVA (Statview) to compare differences in penetrance of phenotypes.

RNA interference of *vab-1*

For dsRNA-mediated interference of *vab-1* a 1.9 kb *Spe*I-*Pst*I fragment of the *vab-1* cDNA was subcloned into the RNAi vector L4440. RNAs were synthesized and annealed as described (Harrington et al., 2002), and injected at a concentration of ~70 ng/μl. Injected hermaphrodites were allowed to recover for 12 hours; eggs laid over the ensuing 24 hours were analyzed. RNAi of *vab-1* resulted in phenotypes approximately half as penetrant as the null mutant (data not shown).

Molecular analysis of *efn-4*

efn-4 corresponds to the predicted gene F56A11.3. cDNAs from this gene had been isolated in a genome-wide cDNA sequencing project (Maeda et al., 2001). The longest cDNA, yk449e2, was sequenced completely; this cDNA lacks the first 11 bases of the predicted coding sequence. The predicted EFN-4 preprotein consists of 348 amino acid residues; an N-terminal signal sequence is predicted to be cleaved after residue A20, and a C-terminal GPI addition signal sequence is predicted to be cleaved near S328. The lesions of the alleles were determined by sequencing genomic DNA from the mutants, as described (George et al., 1998). Sequences of primers are available on request. Using Southern blotting of genomic DNAs and sequencing, we determined that *bx80* is a deletion of 1838 bp, encompassing exon 2 and parts of introns 1 and 2. The breakpoints of *bx80* are: 5′ gttgttaacaacaaaa[*bx80*]aaacctaaatttt 3′.

Transgenic rescue and reporter constructs

To generate a genomic clone containing *efn-4*, we subcloned a 16.1 *Hin*dIII-*Eag*I genomic DNA fragment from cosmid F56A11 into pSL1190, creating pCZ148. This clone contains 5.3 kb genomic sequence 5′ to the EFN-4 ATG. Transgenic lines (*juEx150, juEx152, juEx153*) were made by co-injection of pCZ148 and the marker plasmid pRF4 (both at ~50 ng/μl) in an *efn-4(bx80)* background and the penetrance of the posterior morphology (Vab) phenotypes quantitated in transgenic (Roller) animals. In a typical transgenic line the penetrance of the Vab phenotype was 0.7% (2/300 Rollers were

Vab), compared with 27% in control lines bearing pRF4 alone (*n*=175). To overexpress EFN-4 we also used the transgene *juEx350* described above.

An EFN-4::GFP reporter was constructed by insertion of the GFP intron cassette from vector pPD121.89 into the *Sac* II site of the rescuing genomic clone pCZ148, to create the EFN-4::GFP clone pCZ147. This clone is predicted to encode EFN-4 with GFP inserted in-frame close to the N terminus of the mature protein, after residue 33. Three transgenic lines (*juEx151, juEx205 juEx206*) were established by injection of pCZ148 (40 ng/μl) with the co-injection marker plasmid pRF4, and two lines (*juEx206, juEx210*) formed by co-injection of pCZ147 and the *lin-15(+)* plasmid pLin-15EK into *lin-15(n765)* animals. All EFN-4::GFP transgenic lines yielded similar expression patterns. Chromosomal integrants of *juEx210* (*juIs109* and *juIs110*) were made by X-ray mutagenesis. The lethality of an *efn-4(bx80)* strain is suppressed from ~32% to ~5% by the *juIs109* transgene. Staining with anti-EFN-4 antisera was performed on animals overexpressing EFN-4, either from the EFN-4-GFP array (*juIs109)* or from EFN-4-overexpressing animals (*juEx350*). To examine co-expression of EFN-4-GFP and VAB-1, we established a VAB-1-overexpressing array (*juEx445*) by injection of the *vab-1(+)* cosmid M03A1 (15 ng/μl) and pRF4 (30 ng/μl) into *juIs109*-carrying animals. Co-expression of EFN-1 and EFN-4 was examined by making animals transgenic for *juIs109* and the *efn-1* transgene *juIs53*.

Anti-EFN-4 antibody production

To express EFN-4 in bacterial cells, we cloned DNA encoding amino acid residues 26-325 (i.e. EFN-4 lacking secretion and GPI-addition signal sequences) into pET21a (Novagen), creating the expression clone pICS531. The resulting fusion protein is tagged with 6xHis at the C terminus. EFN-4-6HIS was induced with 0.1 mM IPTG in BL21 (DE3) bacteria and purified on Ni-NTA beads (Qiagen) under denaturing conditions (8 M urea). Purified EFN-4-6HIS was dialyzed in 1×PBS, lyophilized and injected into rabbits for antibody production (Animal Pharm). Anti-EFN-4-HIS6 antibodies were preabsorbed to total protein acetone powders derived from, *E. coli*, HEK 293T and *efn-4(bx80)* protein lysates. Affinity-purified anti-EFN-4 antibodies were kept at a final concentration of 1-5 mg/ml.

Fixation and staining of *C. elegans* embryos were as described (Finney and Ruvkun, 1990). Chicken anti-GFP antibodies (Chemicon), affinity-purified anti-EFN-4, anti-EFN-1 (Chin-Sang et al., 1999), anti-VAB-1 (S. E. G. and A. D. C., unpublished) and MH27 monoclonals (Francis and Waterston, 1991) were used at 1:200 to 1:500 dilution. All fluorescently conjugated secondary antibodies were used at 1:500 dilution in antibody buffer A. Data were collected on a Leica TCS-NT confocal microscope.

Accession Number

The GenBank Accession Number for the *efn-4* cDNA is AF410936.

RESULTS

mab-26 mutations affect EFN-4

EFN-4, encoded by *C. elegans* gene F56A11.3, is a divergent member of the ephrin family of ligands for Eph receptors (Fig.

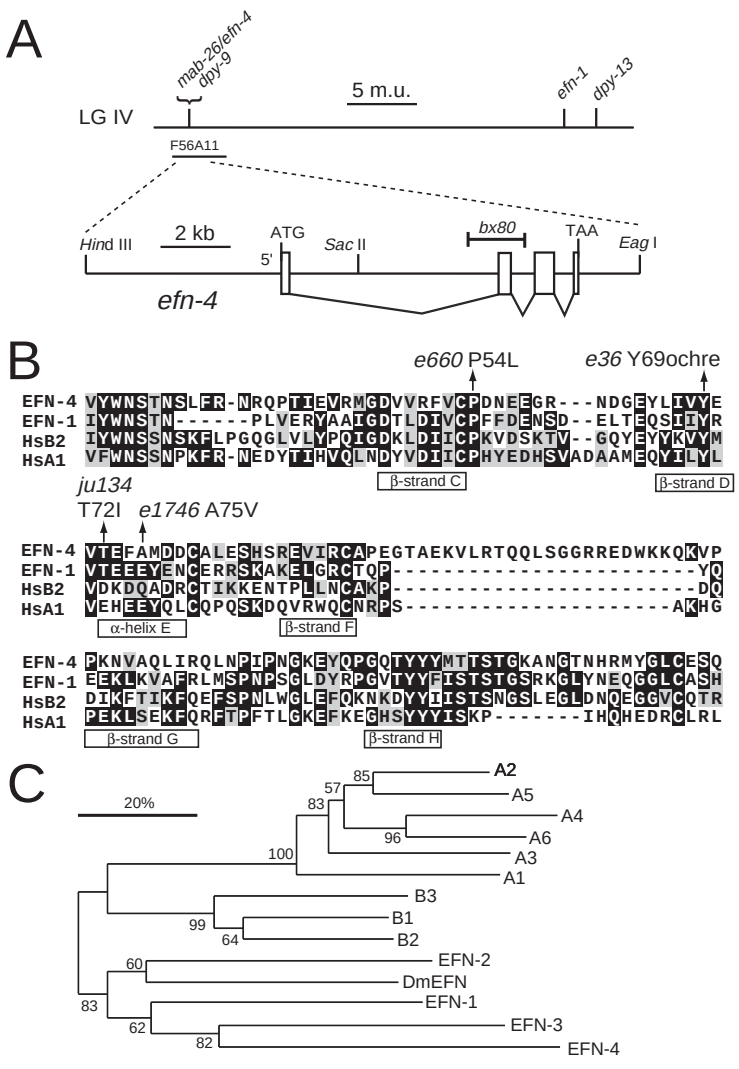

Fig. 1. Structure of the *efn-4* locus and sequence comparisons. (A) Genetic and physical maps of the *efn-4* region. *mab-26/efn-4* is located at the left end of linkage group IV. (B) Alignment of the conserved domain of EFN-4 (residues 25-170) with those of other ephrins, showing point mutations; locations of predicted secondary structure elements are based on structures of ephrin B2 (Toth et al., 2001; Himanen et al., 2001). The ephrin with highest similarity to EFN-4 within the conserved domain is EFN-1 (31% identity, 46% similarity). The EFN-4 conserved domain is approximately equally similar in sequence to the ephrin A and ephrin B subclasses of vertebrate ephrins (25-20% identity; sequences shown are human ephrin A1 and ephrin B2). Alignments were made using ClustalW; identities are in black and similarities in gray. Secondary structure elements are aligned according to Himanen et al. (Himanen et al., 2001). The strong allele *ju134* affects a non-conserved threonine residue; the weaker allele *e660* affects a conserved proline; and the weakest allele, *e1746*, affects a non-conserved alanine residue. When aligned according to Toth et al. (Toth et al., 2001) *ju134* affects an exposed residue of β-strand D, which may play a role in ephrin dimerization; *e660* affects a residue at the end of β-strand C in the tetramerization interface; and *e1746* affects a buried residue between β-strand D and α-helix E. (C) Phylogenetic tree of *C. elegans*, *Drosophila* and vertebrate ephrin sequences. Phylogenetic analysis suggests that the *C. elegans* ephrins diverged after the last common ancestor of vertebrates and nematodes; among the *C. elegans* ephrins, EFN-4 is the most rapidly evolving. Vertebrate ephrin sequences used are from humans except for ephrin A6 (chick). This tree was generated using a neighbor-joining algorithm (MEGA); bootstrap values are indicated at branches.

Table 1. *efn-4* alleles and molecular lesions

Allele	Embryonic arrest (%)	Larval arrest (%)	Adult, Vab (%)	Adult, non-Vab (%)	Wild-type sequence	Mutant sequence	Effect
bx80	14.1	18.8	12.6	54.4	–	–	1838 bp deletion of exon 2
ju134	15.2	10.0	20.2	54.4	ACC	ATC	T72I
e36	11.1	10.5	17.7	60.6	TAT	TAA	Y69ochre
e660	7.0	5.2	21.4	66.4	CCG	CTG	P54L
e1746	3.6	5.7	18.6	72.0	GCG	GTG	A75V

1) (Wang et al., 1999). Like other *C. elegans* ephrins, EFN-4 shows similarities to both trans-membrane and GPI-anchored vertebrate ephrins within its receptor-binding domain (Fig. 1B). However, the conserved domain of EFN-4 also contains a 21-residue insertion relative to other ephrins (Fig. 1B); this insert is predicted to affect a loop between β-strands F and G of the ephrin crystal structure (Toth et al., 2001). Phylogenetic analysis suggests that EFN-4 is a rapidly diverging member of the *C. elegans* ephrin family (Fig. 1C).

We reasoned that mutations in *efn-4* might cause defects in epidermal morphogenesis similar to those caused by mutations in the VAB-1 Eph receptor or the EFN-1 ephrin. The *mab-26(bx80)* mutation, identified on the basis of male tail morphogenetic defects (Chow and Emmons, 1994), causes variable defects in epidermal morphology throughout the body, and maps to the same genomic region as *efn-4* (Fig. 1A). We found that a 16.1 kb genomic DNA clone (pCZ148) containing the *efn-4* locus completely rescued all *mab-26(bx80)* phenotypes in transgenic lines (see Materials and Methods). The *bx80* mutation is a 1.8 kb deletion in *efn-4*, and four additional *mab-26* alleles result from point mutations in this gene, confirming that *efn-4* corresponds to *mab-26*; we subsequently refer to this gene as *efn-4*. All five *efn-4* mutations are recessive and cause similar morphogenetic

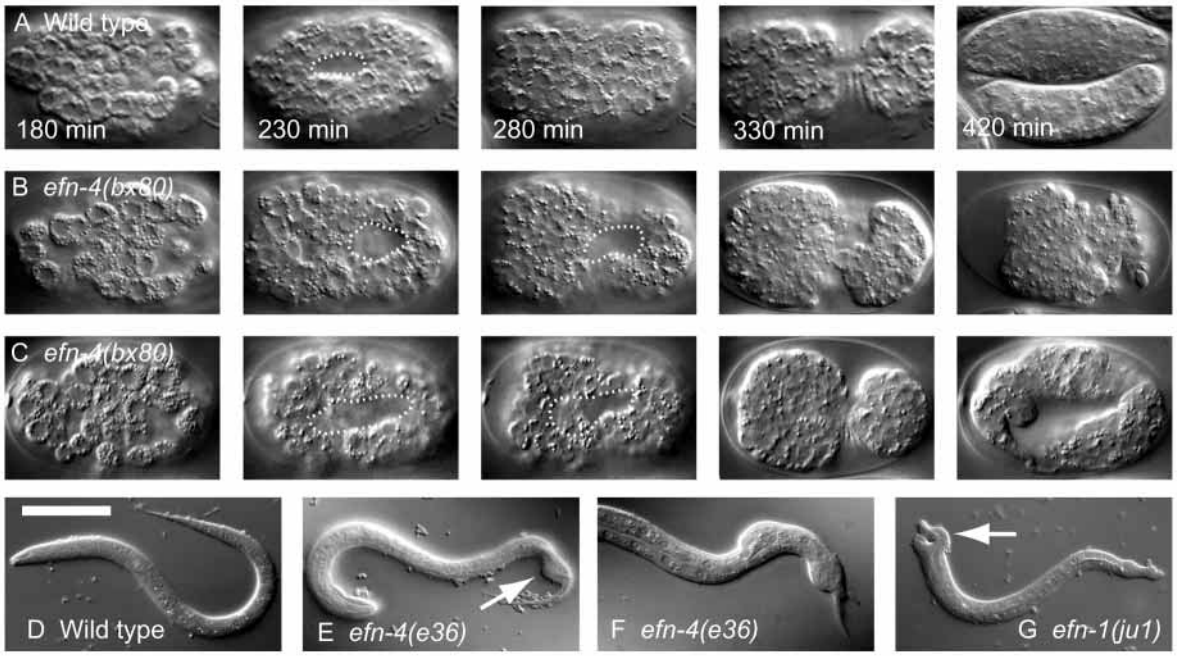

Fig. 2. *efn-4* embryonic and larval phenotypes. Frames from 4D Nomarski DIC movies of individual embryos are shown; all embryos are shown as ventral views; times are relative to first cleavage and are the same for all genotypes. Scale bar: 20 μm in A-C; 50 μm in D-G. (A) Embryogenesis of wild type (N2), ventral views. Note complete closure of the ventral gastrulation cleft (outlined) by 280 minutes. (B,C) Frames from movies of two representative *efn-4(bx80)* embryos, showing enlarged ventral gastrulation clefts. A total of 58 *efn-4(bx80)* and 36 *efn-4(e36)* embryos were recorded for 4D analysis; the range and penetrance of phenotypes was similar in both mutants and the data are considered together below. Some phenotypes of *efn-4* embryos could be classified using the same phenotypic classes as used to classify *vab-1* and *efn-1* phenotypes (George et al., 1998; Chin-Sang et al., 1999). Twenty percent (19/94) of *efn-4* animals displayed the Class I phenotype shown in B, in which the gastrulation cleft was enlarged and persistent (dotted outline, 230-280 minutes), the epidermis failed to enclose and internal cells ruptured during early enclosure (330 minutes); this phenotype is seen in 19% of *vab-1(0)* animals and 12% of *efn-1* animals. Three out of 94 animals exhibited a slightly weaker phenotype resembling the *vab-1* Class II phenotype (enlarged gastrulation cleft; epidermis encloses, embryo turns then ruptures). One out of 94 *efn-4* embryos displayed normal gastrulation clefts and arrested during elongation (*vab-1* Class III phenotype), compared with 38% of *vab-1* or 16% *efn-1* embryos. Sixty-one out of 94 *efn-4* embryos displayed the phenotype shown in C, in which the gastrulation cleft was transiently enlarged (230-280 minutes) and later closed; epidermal enclosure and elongation occurred with normal timing, and the embryo hatched with deformations in the posterior epidermis. Ten out of 94 embryos displayed wild-type development. (D-G) L1 larvae, showing wild type (D), *efn-4(e36)* mutant tail morphology (arrow, E,F) and *efn-1(ju1)* Notch head morphology (arrow, G).

defects (Table 1; Fig. 2). The three strongest alleles (*bx80*, *e36*, and *ju134*) probably abolish *efn-4* function.

When expressed in human 293T cells, EFN-4 is localized to the cell surface, as detected with anti-EFN-4 antibodies (data not shown). In experiments using VAB-1-AP fusion proteins to determine the affinity of VAB-1/EFN-4 interactions, as previously described (Chin-Sang et al., 1999), we were unable to detect binding of VAB-1-AP (10 nM) to EFN-4-expressing cells. These data are consistent with previous evidence that the VAB-1/EFN-4 interaction may be weak (Wang et al., 1999) relative to other VAB-1/EFN interactions.

EFN-4 regulates embryonic neuroblast movements and epidermal morphogenesis

efn-4(bx80) mutants display defects in the morphogenesis of post-embryonic male tail sensilla (Chow and Emmons, 1994; Hahn and Emmons, 2002). *efn-4* mutants also have widespread defects in embryonic morphogenesis of the posterior body: about 20-30% of *efn-4* larvae and adults have blunted or mis-shapen posteriors (Fig. 2E,F), although the head morphology defects ('Notched head'; Fig. 2G) of *vab-1* or *efn-1* mutants (George et al., 1998; Chin-Sang et al., 1999) are rarely seen in *efn-4* mutants. In general the post-embryonic phenotypes of *efn-4* mutants partly overlap those of *vab-1* or *efn-1* mutants.

The posterior morphology defects of *efn-4* mutants arise during embryogenesis. We analyzed the development of *efn-4* embryos using four-dimensional (4D) time-lapse microscopy and found that *efn-4* mutants displayed defects in the same embryonic morphogenetic processes as are affected in *vab-1*: neuroblast movements during closure of the ventral gastrulation cleft, and enclosure of the epidermis (George et al., 1998; Chin-Sang et al., 1999). Although some embryonic defects of some *efn-4* mutants could be classified according to the criteria used previously in our analyses of *vab-1* and *efn-1*, we also observed additional phenotypic classes, detailed below.

Almost all *efn-4* mutant embryos displayed an enlarged and persistent gastrulation cleft (Fig. 2B,C, 230 and 280 minutes); by contrast, *vab-1* or *vab-2* mutants display a much lower penetrance of enlarged clefts. In wild-type development, the gastrulation cleft is 1-2 μm deep and remains visible as a gap in the ventral neuroblast sheet for ~30 minutes to 1 hour (Fig. 2A, 230 min). By contrast, the gastrulation cleft in *efn-4* mutants varies between 2 μm and 10 μm in depth (n=94), and persists for longer than in the wild type. About 20% of *efn-4* embryos displayed an enlarged gastrulation cleft that remained open until the time of epidermal leading cell migration, resulting in a failure of epidermal enclosure and rupture at the ventral midline, as shown in Fig. 2B; this phenotype resembles the Class I phenotype of *vab-1* or *efn-1* mutants. In contrast to *vab-1* or *efn-1* mutants, which frequently rupture during epidermal elongation (*vab-1* class IV), less than 1% of *efn-4* embryos arrested in later embryogenesis. Most *efn-4* embryos (65%) displayed a novel phenotype in which the gastrulation cleft was enlarged and delayed in closing, yet epidermal enclosure and elongation proceeded normally; such animals hatch with normal morphology or defective posterior morphology (Fig. 2C). Six percent of *efn-1* animals display similar transient abnormalities in the gastrulation cleft that do not result in later epidermal rupture (Chin-Sang et al., 1999). In summary, although there is some overlap, the spectrum of embryonic defects in *efn-4* mutants is different from that seen in *vab-1* or *efn-1* mutants.

EFN-4 is expressed in the developing nervous system

To determine the expression pattern of EFN-4 we generated anti-EFN-4 antisera; these antisera were able to detect EFN- 4 in animals overexpressing EFN-4 although not in wild-type animals. We also examined the expression of a functional EFN-4::GFP reporter construct (see Materials and Methods). We observed indistinguishable expression patterns using both methods.

We first detected EFN-4 at about the 100-cell stage in a large number of ventral surface cells, identified as neural or epidermal precursors (Fig. 3E). During and after enclosure of the epidermis, EFN-4 was expressed in many neurons and not in epidermal cells (Fig. 3A-C). In later embryos, larvae and adults, EFN-4-GFP was expressed in several head neurons, pharyngeal cells and a small number of lateral and tail neurons, within which EFN-4 was localized throughout the neuronal cell body and in axonal processes (Fig. 3M-O). When compared with the expression pattern of EFN-1, EFN-4 expression is relatively widespread (Fig. 3D-I) and only overlapping in part.

If EFN-4 is a cell-surface ligand for VAB-1 then it should be expressed at least in part in cells that contact VAB-1-expressing cells. Our data show that this is the case. During epidermal enclosure, EFN-4- and VAB-1-expressing cells are widely distributed in the ectoderm, allowing many possible points of contact (Fig. 3J-L). We conclude that EFN-4 expression in embryos is consistent with the possibility that it interacts with VAB-1; interestingly, some cells appear to express both VAB-1 and EFN-4 (e.g. circled cell in Fig. 3J-L).

efn-4 mutations enhance *vab-1* (Eph receptor) null phenotypes and are synthetic-lethal with weak *vab-1* mutations

We reasoned that if *efn-4* functions only in the same pathway as the VAB-1 Eph receptor, then the phenotype of a VAB-1 receptor null mutant [*vab-1(0)*] should not be enhanced by loss of EFN-4. Alternatively, if EFN-4 has functions that are independent of the VAB-1 receptor, then a *vab-1(0); efn-4* double mutant might be enhanced relative to a *vab-1(0)* mutant. We constructed strains doubly mutant for *vab-1* and *efn-4*, and found that *efn-4* mutations enhanced *vab-1* null alleles. All *vab-1; efn-4* double mutants displayed dramatically enhanced lethality relative to the single mutants, and were maintained as balanced strains for phenotypic analysis (see Materials and Methods). Most *vab-1(0); efn-4(0)* double mutant animals showed the embryonic-lethal phenotype shown in Fig.4A, which is more severe than observed in either *vab-1* or *efn-4* single mutants, in that the gastrulation cleft is deeper (average ~10 μm, n=19) and the entire embryo appears mildly disorganized.

VAB-1 has both kinase-dependent and kinase-independent functions (George et al., 1998). To determine if *efn-4* mutations synergized with either or both functions, we compared the phenotypes of *vab-1(0) efn-4* double mutants with those of *vab-1(kinase) efn-4* double mutants. We found that *vab-1(kinase); efn-4(0)* double mutants displayed strong synergistic phenotypes that were nevertheless weaker than those of *vab-1(0); efn-4(0)* double mutants (compare Fig. 4A

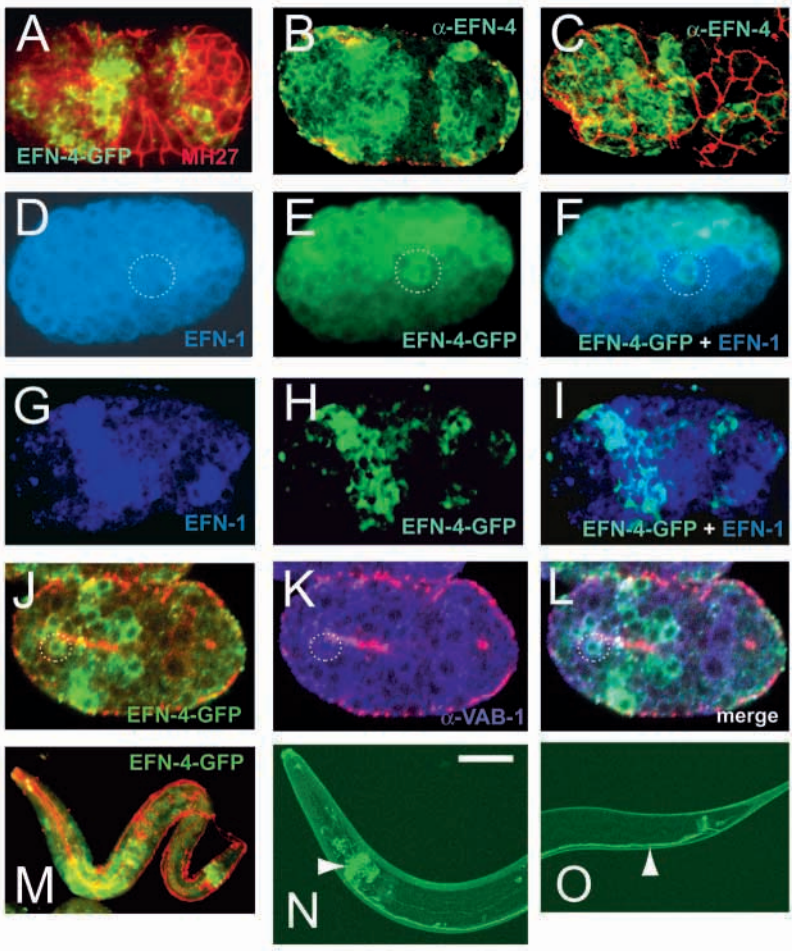

Fig. 3. Expression pattern of EFN-4. (A-C) EFN-4 expression during and after epidermal enclosure, detected using the EFN-4-GFP transgene *juIs109* or in animals overexpressing EFN-4 from the transgene *juEx350*. Genotype in A is *lin-15(n765); juIs109[EFN-4::GFP, lin-15(+)]*, stained with anti-GFP (green) and the monoclonal antibody MH27 to illustrate epidermal adherens junctions (red); ventral view. (B,C) EFN-4 overexpressing embryos, stained with anti-EFN-4 (green) and MH27 (red). B is a confocal midline section at about the same stage as A; C shows a lateral view confocal projection at comma stage, after enclosure. Note the broad distribution of EFN-4-positive cells in the head. Genotype for D-I is *lin-15(n765);EFN-4-GFP(juIs109);EFN-1(juIs53)*, stained with anti-GFP, anti-EFN-1 and MH27. (D-F) In early embryo (~100-cell stage; ventral views). Both EFN-4 and EFN-1 are broadly expressed. The expression of EFN-4 and EFN-1 appears slightly complementary: some cells expressing high levels of EFN-4 (circled) express lower levels of EFN-4, and vice versa. (G-I) Expression of EFN-1 and EFN-4 during late epidermal enclosure, subventral views. EFN-4 expression (green) partly overlaps (yellow) that of EFN-1 (blue). (J-L) Double staining (midline confocal section) of EFN-4-GFP (green) and VAB-1 (purple) during epidermal enclosure. Circle indicates pharyngeal cell expressing EFN-4-GFP and VAB-1. Genotype is *n765; juIs109; juEx445*[*vab-1(+)*], also stained with MH27 antibodies. (M) EFN-4-GFP in L1 stage larva. Double staining with anti-GFP and MH27 antibodies (red). (N,O) EFN-4-GFP expression in late larvae. Note localization of EFN-4-GFP to nerve ring (arrowhead, N) and ventral cord (arrowhead, O). Genotype for M-O is *juIs109*. Scale bar: 10 μm (A-L); 20 μm (M); 50 μm (N,O).

with 4B) suggesting that EFN-4 acts redundantly with both kinase-dependent and kinase-independent functions of *vab-1*. In addition, we constructed strains containing *vab-1* extracellular domain mis-sense mutations (*e699*, *e856*, *e1029* or *ju8*) with either of the hypomorphic *efn-4* mis-sense alleles (*e660* or *e1746*), and found that all eight such double mutant combinations showed synergistic lethality (data not shown). Because the synthetic-lethal interaction of *vab-1* and *efn-4* is allele nonspecific we conclude that *vab-1* and *efn-4* mutations affect parallel, partly redundant pathways.

The synergistic interaction of *efn-4* mutations with mutations in the VAB-1 Eph receptor stands in contrast to *efn-1* mutations, which do not enhance *vab-1(0)* embryonic phenotypes (Chin-Sang et al., 1998) (data shown for comparison in Fig. 5). We therefore asked if other *C. elegans* ephrins showed similar interactions with *vab-1* that might be suggestive of *vab-1*-independent functions. We found that loss of function in *efn-2*, but not in *efn-3*, slightly but significantly enhanced the embryonic and larval lethal phenotypes of a *vab-1* null mutant (Fig. 5). *efn-2* mutants and *vab-1 efn-2* double mutants also displayed a reduced brood size (average=158 progeny) compared with *vab-1* null mutants [average=281 for *vab-1(dx14)*] or other *efn* mutants (data not shown); we have not investigated the basis for the reduced fertility of *efn-2* strains. We further tested whether *efn-1*, *efn-2* and *efn-3* might have redundant functions in VAB-1-independent pathways using *vab-1* dsRNAi (see Materials and Methods) in an *efn-1 efn-2 efn-3* triple mutant background. Such *vab-1(RNAi) efn-1,2,3* quadruple-mutant embryos displayed morphogenetic defects similar in range and penetrance to the *efn-1,2,3* triple mutant (data not shown). Although this experiment is subject to the caveat that RNAi does not fully abolish *vab-1* function, we provisionally conclude that *efn-1*, *efn-2* and *efn-3* are unlikely to function redundantly in VAB-1-independent processes in morphogenesis.

efn-4 mutations are synthetic-lethal with *ptp-3* mutations

Mutations in the LAR-like receptor tyrosine phosphatase *ptp-3* cause low-penetrance defects in neural and epidermal morphogenesis and also show synergistic interactions with *vab-1* and *efn-1* mutations (Harrington et al., 2002) that are, in general, weaker than those of *efn-4* mutations. The similarity of the *ptp-3* and *efn-4* phenotypes and genetic interactions led us to test whether *ptp-3* might function in the same pathway as *efn-4*. We found that *ptp-3; efn-4* double mutants displayed a fully penetrant synergistic embryonic lethality, inconsistent with PTP-3 functioning in a linear pathway with EFN-4 (Fig. 4C). *vab-1(0) ptp-3; efn-4* triple mutant embryos displayed abnormal gastrulation clefts that were larger than in *vab-1(0) efn-4* or *ptp-3 efn-4* double mutants (compare outlines in Fig. 4D with 4A and 4C; see legend to Fig. 4 for quantitation of gastrulation cleft morphology). Such triple mutant embryos appeared qualitatively more abnormal than the double mutants,

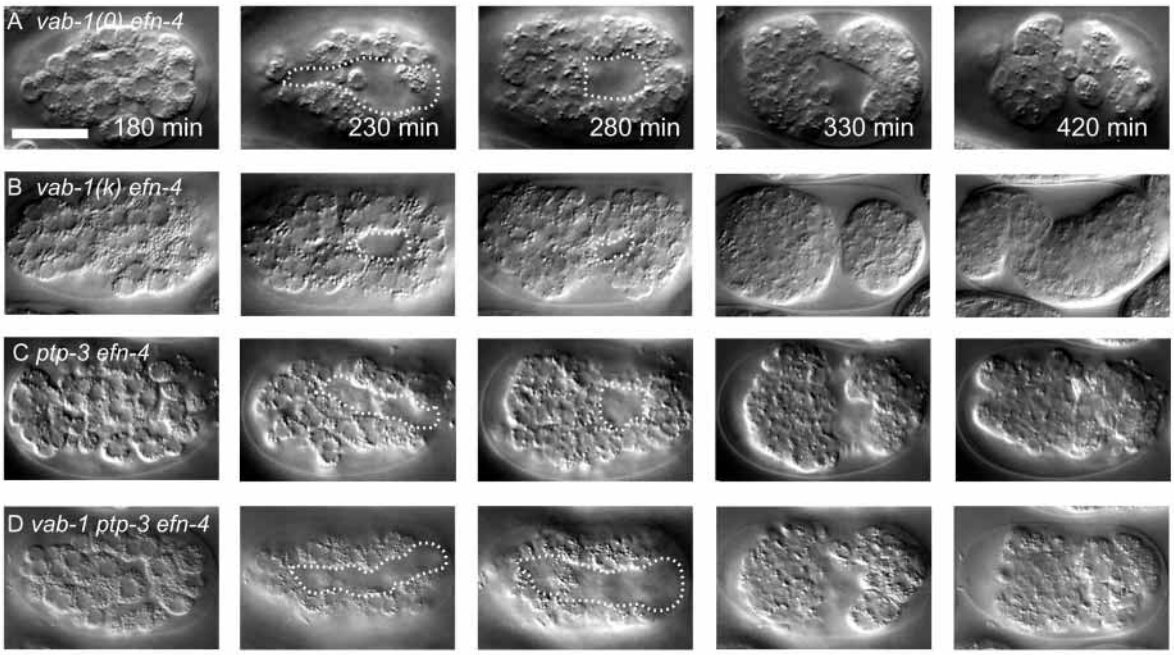

Fig. 4. Embryogenesis of *efn-4; vab-1* and *efn-4 ptp-3* double mutants and *vab-1 ptp-3 efn-4* triple mutant. Frames from 4D Nomarski DIC movies of individual embryos are shown; all embryos are shown as ventral views; times are relative to first cleavage and are the same for all genotypes. (A) Typical *vab-1(0) efn-4(0)* double mutant; open gastrulation cleft at 230-280 minutes is outlined. Nineteen *vab-1(0) efn-4(0)* double mutant embryos were recorded from strain CZ2251, genotype *vab-1(e2027)/mIn1 mIs14; efn-4(bx80)*. Twelve out of 19 were more severely defective than the typical *vab-1* Class I phenotype: the gastrulation cleft was deeper and did not close; cells also appeared loose and disorganized throughout the embryo, and the epidermis failed to enclose. Six out of 16 displayed enlarged gastrulation clefts, underwent epidermal enclosure and ruptured at 1.5-fold stage of elongation; one out of 19 displayed a *vab-1* Class III phenotype (normal gastrulation cleft, rupture at twofold stage). (B) *vab-1(kinase) efn-4* double mutant, genotype *vab-1(e118); efn-4(bx80)*, showing transiently enlarged gastrulation cleft and elongation stage arrest; this phenotype resembles a combination of the most common *efn-4* phenotype and the *vab-1* Class III phenotype. Seventeen *vab-1(kinase) efn-4* double mutant embryos were recorded. The embryo shown is from strain CZ2252, genotype *vab-1(e118)/mIn1 mIs14; efn-4(bx80)*. Four non-GFP-expressing embryos were recorded, of which one displayed a severe Class I phenotype; three displayed milder gastrulation cleft defects and arrested at the twofold stage. Embryos were also recorded from strain CZ1944, genotype *vab-1(e116); efn-4(bx80); juEx350[vab-1(+) efn-4(+)]*. Thirteen embryos were recorded that had lost the array (judged from absence of GFP expression). Of the thirteen, five displayed a typical Class I phenotype, six arrested at the 1.5-fold stage (Class II-like), and two arrested later in elongation (Class III). We also recorded four *vab-1(ecd) efn-4* double mutants from strain CZ2249, genotype *vab-1(e200)/mIn1 mIs14; efn-4(e36)*. Three out of four displayed a severe Class I phenotype and one displayed a Class IV-like phenotype. (C) *ptp-3(op147); efn-4(bx80)* double mutant, showing Class I phenotype. Twelve out of 12 *ptp-3(op147); efn-4(bx80)* embryos recorded showed similar phenotypes. Measured as a percentage of the embryo at the maximum extent of the cleft, the gastrulation clefts in the double mutants extended to 30-50% of embryonic width; 50-100% of embryonic length, and were on average 8 μm deep at their maximum extent. (D) *vab-1(dx31) ptp-3(op147); efn-4(bx80)* triple mutant, illustrating extreme Class I phenotype and disorganization of embryonic blast cells during gastrulation. All of the 16 such embryos showed the phenotypes illustrated. Gastrulation clefts in these triple mutants extended to 50-75% of embryonic width; 75-90% of embryonic length, and were on average10 μm deep. Scale bar: 20 μm.

in that cells were more mobile and less tightly packed in the embryo. Because *vab-1 ptp-3 efn-4* triple mutants appeared more severely affected than *vab-1 ptp-3*, *vab-1 efn-4* or *ptp-3 efn-4* double mutants, these data suggest that VAB-1, PTP-3 and EFN-4 may function in distinct yet partly redundant pathways in embryonic morphogenesis.

EFN-4 and MAB-20 Semaphorin-2A may function in common or opposing pathways in early embryonic morphogenesis

Loss of function of the *C. elegans* secreted Semaphorin-2A homolog MAB-20 causes defects in male tail morphogenesis (Baird et al., 1991) similar to those of *efn-4* mutants. It has been suggested that these two genes might affect a common pathway in male tail development (Chow and Emmons, 1994; Roy et al., 2000). To ask whether *mab-20* and *efn-4* might function in the same pathway in embryogenesis, we examined the embryonic morphogenetic defects of *mab-20* mutants using 4D analysis. We found that *mab-20* mutants were frequently defective in closure of the gastrulation cleft (Fig. 6A, arrow at 230 minutes); in general, the defects resembled those seen in *efn-4* mutants. Thus, in addition to its role in enclosure of the posterior epidermis, semaphorin signaling is also involved in the earlier process of neuroblast migration.

We examined the consequences of reducing both MAB-20 signaling and ephrin signaling on embryonic morphogenesis. We made several *mab-20 efn-4* double mutant strains using either null or weak alleles of either gene. In contrast to *vab-1*, *efn-1* or *ptp-3* mutations, *mab-20* mutations did not show synthetic-lethal interactions with *efn-4* mutations. In all *mab-20 efn-4* double mutant strains the penetrance of

embryonic lethality was not significantly different from that of the corresponding *mab-20* single mutants (Fig. 7A). Using 4D microscopy, we confirmed that most *mab-20 efn-4* double mutant embryos showed morphogenetic defects that were less severe than expected from additivity of the single mutants. In particular, the gastrulation cleft defects of *mab-20 efn-4* double mutants were sometimes less severe than in either single mutant (Fig. 6C,D). The less than additive effect of *mab-20* and *efn-4* in embryonic morphogenesis suggests that these two genes might either have antagonistic roles or that they might operate in a common pathway.

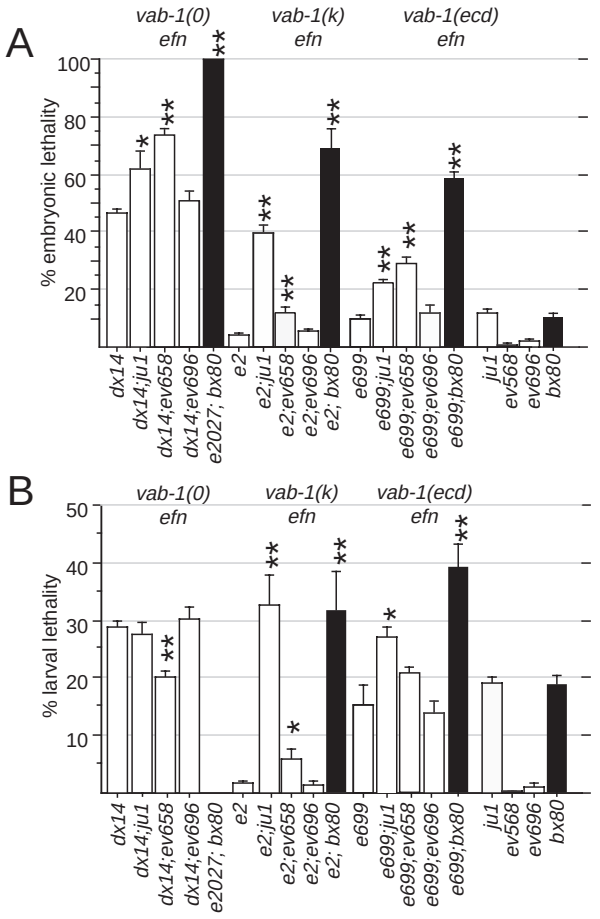

Fig. 5. Quantitation of embryonic (A) and larval (B) lethality in *vab-1 efn* double mutants. *vab-1; efn* double mutants were constructed and lethality quantitated as described in the Materials and Methods. All *vab-1; efn*-4 double mutants (black bars) showed significantly enhanced lethality compared with the relevant single mutants (white bars). vab-*1(0); efn-4* double mutants were fully lethal and maintained as balanced strains of genotype *vab-1/mIn1 mIs14; efn-4*. *vab-1(e2); efn-4* and *vab-1(e699); efn-4* double mutants were >96% lethal, with rare escapers; among these escapers, 30-50% were fertile with average brood sizes of 24 and 51, respectively. Data for *vab-1; efn-1* double mutants, included for comparison, are taken from Chin-Sang et al. (Chin-Sang et al., 1998). *efn-2* mutations significantly increase the embryonic lethality and significantly decrease the larval lethality of *vab-1(0)* mutants. *efn-2* mutations also significantly enhanced the embryonic and larval lethal phenotypes of *vab-1(kinase)* mutations, a result that contrasts with the lack of enhancement of *vab-1(kinase)* male tail phenotypes by *efn-2* (Wang et al., 1999). *vab-1; efn-3* double mutants were not significantly different from *vab-1* controls. Error bars indicate the s.e.m. Differences in penetrance between *vab-1* and *vab-1; efn* strains were compared using ANOVA; *, $P<0.05$; **, $P<0.01$.

We analyzed later embryonic and larval phenotypes of *mab-20* and *mab-20 efn-4* double mutants to explore further whether *mab-20* and *efn-4* might function in common or opposing pathways later in development. *mab-20* mutants display defects in cell-cell associations in the ventral epidermis, manifested as ectopic contacts between P cells (Roy et al., 2000). *efn-4* mutants displayed normal contacts between ventral P cells during embryogenesis; furthermore, *efn-4* mutations did not suppress the ectopic P cell contacts due to *mab-20* mutations (62/78 *mab-20(ev574) efn-4(e660)* embryos displayed ectopic P cell contacts, compared with 53/75 *mab-20(ev574)* embryos; $P=0.7$, Fisher's exact test). Overall, *mab-20 efn-4* double mutants showed an increased penetrance of larval lethality consistent with additivity of mutant phenotypes (Fig. 7B). We provisionally conclude that *mab-20* and *efn-4* act independently in later development.

DISCUSSION

EFN-4 is a divergent member of the ephrin family

In this paper, we describe the genetic and molecular analysis of the fourth *C. elegans* member of the ephrin family. Although the primary sequence of EFN-4 shows only modest similarity to those of other ephrins, EFN-4 shares all hallmarks of the ephrin family, including a conserved region containing several invariant cysteine and proline residues, and a predicted C-terminal GPI addition signal sequence. The major divergent feature of the EFN-4 sequence is an insertion of 21 residues (relative to vertebrate ephrin A proteins; 24 residues relative to other *C. elegans* ephrins) in the conserved domain.

By reference to the structures of mouse ephrin B2 (Toth et al., 2001) and of the ephrin-B2/EphB2 receptor co-crystal (Himanen et al., 2001), the 21-residue insertion in EFN-4 appears to affect the loop between β-strands F and G. In ephrin B2 this 'F-G loop' contributes to the ligand/receptor binding interface. The F-G loop comprises eight residues in vertebrate ephrin A proteins and five residues in vertebrate ephrin B proteins and other *C. elegans* ephrins, suggesting that an enlarged F-G loop could affect the binding specificity of EFN-4. Residues in β-strand G have also been implicated in binding of vertebrate ephrin-A2 to ADAM metalloproteases (Hattori et al., 2000), suggesting that the EFN-4 insert could affect such an interaction; however, the sequence of the metalloprotease binding site itself is poorly conserved in all worm ephrins. Finally, the adjacent G-H domain [Area II by Toth et al. (Toth et al., 2001)] forms the interface between ephrin monomers in the dimeric crystal structure. An intriguing possibility is that a longer F-G loop might affect ephrin homo- or heterodimerization and thus could allow EFN-4 to act as an inhibitory ephrin. Genetic analysis of ephrin double and triple mutants has not uncovered any evidence for such an antagonistic interaction between *C. elegans* ephrins (S. L. M and A. D. C., unpublished). An alternative possibility, suggested by the apparent receptor-independent nature of EFN-4 function (see below), is that the insert sequence in EFN-4 promotes dimerization in the absence of receptor.

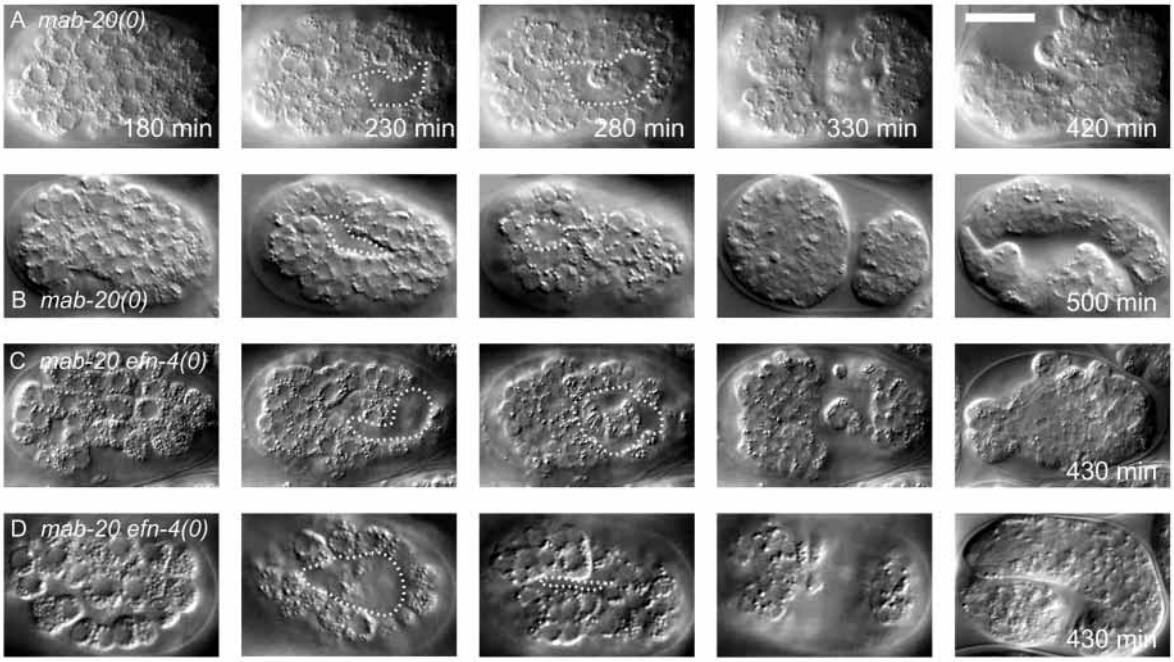

Fig. 6. Gastrulation cleft phenotypes of *mab-20/Semaphorin-2A* mutants and *mab-20 efn-4* double mutants. Frames from 4D Nomarski DIC movies of individual embryos are shown; all embryos are shown as ventral views; times are relative to first cleavage and are the same for all genotypes except where indicated. (A,B) Embryonic morphogenesis of representative *mab-20(ev574)* embryos. Between 180 and 280 minutes post first cleavage, most (28/38) *mab-20(ev574)* embryos displayed a disorganized gastrulation cleft that was deeper and more persistent than in the wild type (A, outlined 230-280 minutes). Of these, about half (13/28) displayed gastrulation clefts that persisted until ventral enclosure; leading epidermal cells failed to enclose and the embryos ruptured at the ventral midline, similar to *efn-4* mutants (compare series A 330 min with Fig. 2 series C). Sixteen percent (6/38) of animals with disorganized gastrulation clefts completed epidermal enclosure and later ruptured at the two- or threefold stage. Eight percent (3/38) closed the gastrulation cleft at the onset of epidermal enclosure, and arrested at the twofold stage of elongation (B, 500 minutes), a phenotype not observed in *efn-4* mutants. Twenty-three percent (9/38) of embryos displayed an enlarged gastrulation cleft yet underwent epidermal enclosure and hatched. (C,D) Morphogenesis of *mab-20(e819); efn-4(bx80)* double mutant embryos. Forty-five percent (16/35) of embryos displayed aberrant gastrulation clefts and either ruptured during ventral enclosure (series C, 430 minutes), arrested during epidermal elongation, or hatched (series D). Cellular disorganization was evident at the onset of gastrulation cleft formation (D, 180 minutes). The terminal phenotypes resembled the most severe *efn-4* or *mab-20* single mutant phenotypes (C, 430 minutes) although the gastrulation cleft was often less open than in *efn-4* (e.g. C, 230-280 minutes). Most (26/35) double mutant embryos hatched, of which one quarter (9/35) displayed gastrulation cleft defects. Typically, the gastrulation cleft remained partly open in the anterior at the onset of epidermal enclosure (outlined in D, 280 minutes) and epidermal enclosure occurred normally (D, 330 minutes). Scale bar: 20 μm.

Evidence that EFN-4 function is not VAB-1-dependent

Several lines of evidence suggest that EFN-4 can function independently of the VAB-1 Eph receptor. First, the *efn-4* mutant phenotype is only partly overlapping with the *vab-1/EphR* null phenotype: in particular, the penetrance of gastrulation cleft defects is significantly higher than seen in *vab-1* strains. Thus, unlike the phenotypes of *efn-1* mutants, which are weaker but otherwise indistinguishable from those of *vab-1*, the *efn-4* phenotypes are distinctly different from those caused by loss of receptor function.

A second line of evidence is the strong synergistic interaction between *vab-1* and *efn-4* mutations. Again, this result contrasts with the other three ephrins: loss of function in *efn-1, efn-2,* or *efn-3* does not exacerbate the phenotypes of *vab-1* null mutants, with one exception. The fully penetrant lethality of a *vab-1(0); efn-4(0)* double mutant could reflect additivity (~80% lethality of a *vab-1* null combined with ~30% lethality of an *efn-4* null), and thus does not by itself imply redundancy of *vab-1* and *efn-4*. However, double mutants made with the weakest alleles of each gene (each resulting in <10% lethality alone) were >99% inviable, suggesting that loss of *efn-4* function strongly sensitizes the animal to loss of *vab-1* function, and vice versa. We propose that *efn-4* and *vab-1* function in parallel pathways that perform related and partly redundant functions in morphogenesis. In support of this, a clear synergistic interaction was also seen in double mutants between *efn-4* and *efn-1*; null mutations in either gene cause ~30% lethality, whereas a double mutant using null alleles was 100% inviable (S. L. M. and A. D. C., unpublished).

A third line of evidence that EFN-4 may not solely signal via VAB-1 is the apparently low affinity of EFN-4/VAB-1 interactions (Wang et al., 1999). The affinity of the VAB-1-EFN-4 interaction appears to be much lower than that of the VAB-1-EFN-1 interaction (K_d ~5 nM) (Chin-Sang et al., 1999). Even if EFN-4 does signal partly via VAB-1, this would not invalidate the conclusion from genetic analysis that EFN-4 also functions in a VAB-1-independent pathway. Genetic and phenotypic analysis suggests that EFN-2 also may have functions independent of VAB-1. Thus, at least two of the four *C. elegans* ephrins appear to have functions that do not require the only known *C. elegans* Eph receptor.

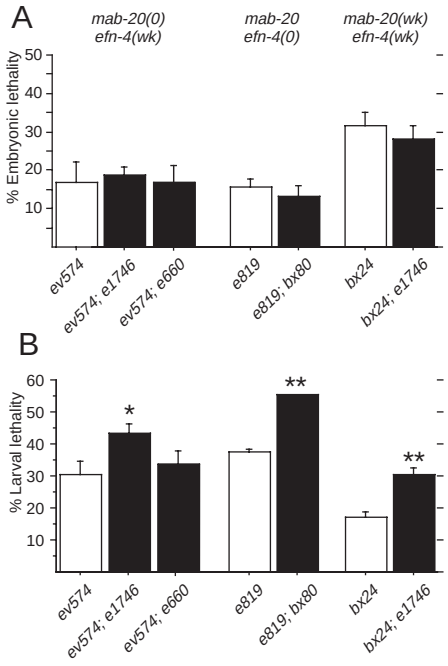

Fig. 7. Quantitation of genetic interactions between *efn-4* and *mab-20.* Penetrance of embryonic lethality (A) and larval lethality (B) in *mab-20* (white bars) and in *mab-20 efn-4* double mutants (black bars). Error bars indicate the s.e.m. Differences in penetrance between *mab-20* and *mab-20; efn-4* strains were compared using ANOVA; *, $P<0.05$; **, $P<0.01$. *mab-20* strains exhibited 20-30% embryonic lethality depending on the allele; in all *mab-20; efn-4* strains, the penetrance of embryonic lethality was not significantly different compared with the *mab-20* single mutant. Most *mab-20; efn-4* double mutant strains displayed significantly increased larval lethality, consistent with additivity of mutant phenotypes.

How might EFN-4 signal in morphogenesis?

We envisage several possibilities for how EFN-4 (and possibly EFN-2) might signal in pathways that do not require the VAB-1 receptor. First, a trivial possibility is that a second Eph-like receptor may exist in the <0.5% of the *C. elegans* genome as yet unsequenced, or that such a receptor may be sufficiently diverged that it is not recognizable using current algorithms. Both these possibilities seem unlikely given the extensive efforts to identify worm kinases (Plowman et al., 1999) and RTKs (Popovici et al., 1999).

Second, EFN-4 may signal via a non-Eph-like receptor. The apparent epistasis of *efn-4* and *mab-20* mutant phenotypes suggests that EFN-4 could signal via a component of the MAB-20 pathway (see below). Vertebrate ephrins can bind ADAM family metalloproteases (Hattori et al., 2000); EFN-4 could signal via one of the *C. elegans* ADAM metalloproteases. Mutations in one such metalloprotease, the kuzbanian ortholog *sup-17* cause complex phenotypes that reflect reduction of *lin-12* and *glp-1* function (Wen et al., 1997); we are currently examining whether *sup-17* plays additional roles in *C. elegans* ephrin signaling. The receptor tyrosine phosphatase PTP-3 also functions in parallel to VAB-1 in morphogenesis (Harrington et al., 2002). However, the Ptp-3 and Efn-4 phenotypes are distinct, and *ptp-3* mutations display strong synergistic interactions with *efn-4* mutations, inconsistent with PTP-3 being the sole EFN-4 receptor. Because *vab-1 ptp-3 efn-4* triple mutant embryos appear only slightly more defective than any corresponding double mutants, our data do not rule out a model in which EFN-4 signals redundantly via VAB-1 or PTP-3. However, in the absence of evidence that EFN-4 directly interacts with either receptor, it is equally possible that VAB-1, EFN-4 and PTP-3 define three partly redundant pathways in morphogenesis.

Third, ephrins form dimers and higher-order multimers (Davis et al., 1994; Toth et al., 2001). Cell culture experiments suggest that co-expression of EFN-4 with EFN-1 does not modulate the ability of EFN-1 to bind VAB-1 (I. D. C.-S. and A. D. C., unpublished), although it could alter the specificity of other ephrins so that a heterodimer could interact with an unknown receptor. Additionally, if VAB-1 does bind EFN-4, the co-expression of VAB-1 and EFN-4 in some cells could alter the responsiveness of VAB-1 to other ligands, as demonstrated for co-expressed ephrins and Eph receptors in vertebrate retinal neurons (Dutting et al., 1999; McLaughlin and O'Leary, 1999).

Finally, EFN-4 might not interact directly with any receptor. Recent data from several groups have suggested that GPI-linked ephrins, like their transmembrane counterparts, can also function as bidirectional signaling proteins (Knoll and Drescher, 2002). Vertebrate Ephrin A proteins may function in reverse signaling as a consequence of their localization to membrane microdomains (Bruckner et al., 1999; Davy et al., 1999; Davy and Robbins, 2000), and *C. elegans* EFN-1 has functions independent of the VAB-1 kinase (Chin-Sang et al., 1999). We speculate that EFN-4 might have evolved to be able to trigger 'reverse signaling' pathways in the absence of receptor binding. For example, the F-G loop insert in EFN-4 might allow it to dimerize more easily than other ephrins, leading to activation of pathways in the absence of the VAB-1 receptor. Further analysis of EFN-4 could provide insights into how GPI-linked ephrins function in bidirectional signaling.

Eph signaling, semaphorin signaling and cell adhesion in the early *C. elegans* embryo

mab-26 (*efn-4*) was proposed to function in the same genetic pathway as the Semaphorin 2A MAB-20, based on the similarity and non-additivity of *mab-20* and *mab-26* mutant phenotypes in male tail morphogenesis (Roy et al., 2000). Consistent with the previous analysis of male tail phenotypes we find that the *efn-4* and *mab-20* embryonic phenotypes are overlapping and show less than additive effects in double mutants. However, our analysis has not conclusively established whether *efn-4* and *mab-20* act in a common pathway in embryogenesis. The apparent epistasis of *mab-20 efn-4* double mutants is also compatible with a model in which *mab-20* and *efn-4* play opposing roles. MAB-20 is ubiquitously expressed in embryos during morphogenesis stages (Roy et al., 2000), rendering possible several kinds of interaction with EFN-4 pathways. Although ephrin and semaphorin pathways both can function in contact-dependent repulsion of axonal growth cones, the consequence of reducing both pathways simultaneously has not been explicitly addressed, and many other combinatorial interactions have been observed between axon guidance pathways (Yu and Bargmann, 2001). Further analysis of genetic interactions between Eph signaling and

semaphorin signaling will be necessary to elucidate their in vivo functional relationships.

Most functions of Eph signaling involve modulation of cell-cell adhesion. Indeed, ephrins were first identified as contact-dependent axon repellents in the vertebrate central nervous system (Cheng et al., 1995; Drescher et al., 1995; Nakamoto et al., 1996). Numerous studies have confirmed and extended this anti-adhesive role of ephrin signaling, both in the nervous system and in non-neuronal cells (Wilkinson, 2001). However, it is clear that in some situations ephrin/Eph signaling can promote cell adhesion (Klein, 2001). The cellular basis for the early embryonic defects of *C. elegans* Eph signaling mutants remains poorly understood, but probably reflects alterations in cell adhesion among neural precursors. The phenotype of *vab-1 ptp-3 efn-4* triple mutants, in which cells appear more mobile than in the wild type, hints that in the *C. elegans* embryo these proteins may function as parts of a redundant cell-adhesion network. However, it remains unresolved whether ephrin signaling directly mediates cell adhesion in the *C. elegans* embryo, or whether it modulates the function of other cell adhesion molecules, such as LAD-1 (Chen et al., 2001).

We thank Jonathan Hodgkin for information regarding unpublished morphological mutants in the Cambridge strain collection, and Xun Huang and Chris Suh for isolating *efn-4* alleles. We thank Yuji Kohara, Andy Fire and the *C. elegans* genome project for clones, vectors and sequence information; Andrew Hahn and Scott Emmons for sharing unpublished results on *efn-4*; Martin Hudson for quantitation of *juIs109* rescue; and Grant Pogson for help with the phylogenetic analysis. We thank David Feldheim, Yishi Jin and members of the Jin and Chisholm laboratories for comments on this manuscript. This work was supported by grants to A. D. C. from the NIH (GM54657), the Alfred P. Sloan Foundation and an NSF Instrumentation Award; by a University of California Biotechnology training grant (to S. E. G.); and by a Human Frontiers Science Program postdoctoral fellowship (I. C.-S.)

REFERENCES

Baird, S. E., Fitch, D. H., Kassem, I. A. and Emmons, S. W. (1991). Pattern formation in the nematode epidermis: determination of the arrangement of peripheral sense organs in the *C. elegans* male tail. *Development* **113**, 515-526.

Brenner, S. (1974). The genetics of *Caenorhabditis elegans. Genetics* **77**, 71-94.

Bruckner, K., Pablo Labrador, J., Scheiffele, P., Herb, A., Seeburg, P. H. and Klein, R. (1999). EphrinB ligands recruit GRIP family PDZ adaptor proteins into raft membrane microdomains. *Neuron* **22**, 511-524.

Chen, L., Ong, B. and Bennett, V. (2001). LAD-1, the *Caenorhabditis elegans* L1CAM homologue, participates in embryonic and gonadal morphogenesis and is a substrate for fibroblast growth factor receptor pathway-dependent phosphotyrosine-based signaling. *J. Cell Biol.* **154**, 841-855.

Cheng, H.-J., Nakamoto, M., Bergemann, A. D. and Flanagan, J. G. (1995). Complementary gradients in expression and binding of ELF-1 and Mek4 in development of the topographic retinotectal projection map. *Cell* **82**, 371-381.

Chin-Sang, I. D. and Chisholm, A. D. (2000). Form of the worm: genetics of epidermal morphogenesis in *C. elegans*. *Trends Genet.* **16**, 544-551.

Chin-Sang, I. D., George, S. E., Ding, M., Moseley, S. L., Lynch, A. S. and Chisholm, A. D. (1999). The ephrin VAB-2/EFN-1 functions in neuronal signaling to regulate epidermal morphogenesis in *C. elegans*. *Cell* **99**, 781-790.

Chow, K. L. and Emmons, S. W. (1994). HOM-C/Hox genes and four interacting loci determine the morphogenetic properties of single cells in the nematode male tail. *Development* **120**, 2579-2592.

Davis, S., Gale, N. W., Aldrich, T. H., Maisonpierre, P. C., Lhotak, V., Pawson, T., Goldfarb, M. and Yancopoulos, G. D. (1994). Ligands for the EPH-related receptor tyrosine kinases that require membrane attachment or clustering for activity. *Science* **266**, 816-819.

Davy, A., Gale, N. W., Murray, E. W., Klinghoffer, R. A., Soriano, P., Feuerstein, C. and Robbins, S. M. (1999). Compartmentalized signaling by GPI-anchored ephrin-A5 requires the Fyn tyrosine kinase to regulate cellular adhesion. *Genes Dev.* **13**, 3125-3135.

Davy, A. and Robbins, S. M. (2000). Ephrin-A5 modulates cell adhesion and morphology in an integrin- dependent manner. *EMBO J.* **19**, 5396-5405.

Drescher, U., Kremoser, C., Handwerker, C., Loschinger, J., Noda, M. and Bonhoeffer, F. (1995). In vitro guidance of retinal ganglion cell axons by RAGS, a 25 kDa tectal protein related to ligands for Eph receptor tyrosine kinases. *Cell* **82**, 359-370.

Dutting, D., Handwerker, C. and Drescher, U. (1999). Topographic targeting and pathfinding errors of retinal axons following overexpression of ephrinA ligands on retinal ganglion cell axons. *Dev. Biol.* **216**, 297-311.

Edgley, M. L. and Riddle, D. L. (2001). LG II balancer chromosomes in *Caenorhabditis elegans*: *mT1(II;III)* and the *mIn1* set of dominantly and recessively marked inversions. *Mol. Genet. Genomics* **266**, 385-395.

Finney, M. and Ruvkun, G. (1990). The *unc-86* gene product couples cell lineage and cell identity in *C. elegans*. *Cell* **63**, 895-905.

Francis, G. R. and Waterston, R. H. (1991). Muscle cell attachment in *Caenorhabditis elegans*. *J. Cell Biol.* **114**, 465-479.

George, S. E., Simokat, K., Hardin, J. and Chisholm, A. D. (1998). The VAB-1 Eph receptor tyrosine kinase functions in neural and epithelial morphogenesis in *C. elegans*. *Cell* **92**, 633-643.

Hahn, A. C. and Emmons, S. W. (2002). The roles of an ephrin and semaphorin in patterning cell-cell contacts in *C. elegans* sensory organ development. *Dev. Biol.* (in press).

Harrington, R. J., Gutch, M. J., Hengartner, M. O., Tonks, N. K. and Chisholm, A. D. (2002). The *C. elegans* LAR-like receptor tyrosine phosphatase PTP-3 and the VAB-1 Eph receptor tyrosine kinase have partly redundant functions in morphogenesis. *Development* **129**, 2141-2153.

Hattori, M., Osterfield, M. and Flanagan, J. G. (2000). Regulated cleavage of a contact-mediated axon repellent. *Science* **289**, 1360-1365.

Himanen, J. P., Rajashankar, K. R., Lackmann, M., Cowan, C. A., Henkemeyer, M. and Nikolov, D. B. (2001). Crystal structure of an Eph receptor-ephrin complex. *Nature* **414**, 933-938.

Klein, R. (2001). Excitatory Eph receptors and adhesive ephrin ligands. *Curr. Opin. Cell Biol.* **13**, 196-203.

Knoll, B. and Drescher, U. (2002). Ephrin-As as receptors in topographic projections. *Trends Neurosci.* **25**, 145-149.

Maeda, I., Kohara, Y., Yamamoto, M. and Sugimoto, A. (2002). Large-scale analysis of gene function in Cenorhabditis elegans by high-throughput RNAi. *Curr. Biol.* **11**, 171-176.

McLaughlin, T. and O'Leary, D. D. (1999). Functional consequences of coincident expression of EphA receptors and ephrin-A ligands. *Neuron* **22**, 636-639.

Mellitzer, G., Xu, Q. and Wilkinson, D. G. (1999). Eph receptors and ephrins restrict cell intermingling and communication. *Nature* **400**, 77-81.

Michaux, G., Legouis, R. and Labouesse, M. (2001). Epithelial biology: lessons from *Caenorhabditis elegans*. *Gene* **277**, 83-100.

Nakamoto, M., Cheng, H. J., Friedman, G. C., McLaughlin, T., Hansen, M. J., Yoon, C. H., O'Leary, D. D. and Flanagan, J. G. (1996). Topographically specific effects of ELF-1 on retinal axon guidance in vitro and retinal axon mapping in vivo. *Cell* **86**, 755-766.

Plowman, G. D., Sudarsanam, S., Bingham, J., Whyte, D. and Hunter, T. (1999). The protein kinases of *Caenorhabditis elegans*: a model for signal transduction in multicellular organisms. *Proc. Natl. Acad. Sci. USA* **96**, 13603-13610.

Popovici, C., Roubin, R., Coulier, F., Pontarotti, P. and Birnbaum, D. (1999). The family of *Caenorhabditis elegans* tyrosine kinase receptors: similarities and differences with mammalian receptors. *Genome Res.* **9**, 1026-1039.

Raich, W. B., Agbunag, C. and Hardin, J. (1999). Rapid epithelial-sheet sealing in the *Caenorhabditis elegans* embryo requires cadherin-dependent filopodial priming. *Curr. Biol.* **9**, 1139-1146.

Riddle, D., Blumenthal, T., Meyer, B. J. and Priess, J. R. (1997). *C. elegans* II. Cold Spring Harbor, NY: Cold Spring Harbor Laboratory Press.

Roy, P. J., Zheng, H., Warren, C. E. and Culotti, J. G. (2000). *mab-20*

encodes Semaphorin-2a and is required to prevent ectopic cell contacts during epidermal morphogenesis in *Caenorhabditis elegans*. *Development* **127**, 755-767.

Simske, J. S. and Hardin, J. (2001). Getting into shape: epidermal morphogenesis in *Caenorhabditis elegans* embryos. *BioEssays* **23**, 12-23.

Toth, J., Cutforth, T., Gelinas, A. D., Bethoney, K. A., Bard, J. and Harrison, C. J. (2001). Crystal structure of an ephrin ectodomain. *Dev. Cell* **1**, 83-92.

Wang, X., Roy, P. J., Holland, S. J., Zhang, L. W., Culotti, J. G. and Pawson, T. (1999). Multiple ephrins control cell organization in *C. elegans* using kinase-dependent and -independent functions of the VAB-1 Eph receptor. *Mol. Cell* **4**, 903-913.

Wen, C., Metzstein, M. M. and Greenwald, I. (1997). SUP-17, a *Caenorhabditis elegans* ADAM protein related to *Drosophila* KUZBANIAN, and its role in LIN-12/NOTCH signalling. *Development* **124**, 4759-4767.

Wilkinson, D. G. (2001). Multiple roles of EPH receptors and ephrins in neural development. *Nat. Rev. Neurosci.* **2**, 155-164.

Williams-Masson, E. M., Malik, A. N. and Hardin, J. (1997). An actin-mediated two-step mechanism is required for ventral enclosure of the *C. elegans* hypodermis. *Development* **124**, 2889-2901.

Xu, Q., Mellitzer, G. and Wilkinson, D. G. (2000). Roles of Eph receptors and ephrins in segmental patterning. *Philos. Trans. R. Soc. Lond. B Biol. Sci.* **355**, 993-1002.

Yu, T. W. and Bargmann, C. I. (2001). Dynamic regulation of axon guidance. *Nat. Neurosci.* **4 Suppl.**, 1169-1176.